İSTANBUL UNIVERSITY
CERRAHPAŞA

ORIGINAL ARTICLE
Electrica 2025; 25: 1-9

Enhancing the Initial Position Estimation of a Resolver in a Servo-Motor-Controlled Satellite Ground Station With Regression Techniques

Yasin Sancar[1], **Ramiz Görkem Birdal**[2]

[1]Department of Information Processing, Atatürk University Open Education Faculty, Erzurum, Türkiye
[2]Department of Computer Engineering, İstanbul University-Cerrahpaşa Faculty of Engineering, İstanbul, Türkiye

Cite this article as: Y. Sancar and R. Görkem Birdal, "Enhancing the initial position estimation of a resolver in a servo-motor-controlled satellite ground station with regression techniques," *Electrica*, 25, 0167, 2025. doi:10.5152/electrica.2025.24167.

WHAT IS ALREADY KNOWN ON THIS TOPIC?

- *Resolvers are commonly used in Low Earth Orbit (LEO) satellite ground stations for precise angular position feedback, but they often suffer from calibration errors due to mechanical misalignments and environmental fluctuations.*
- *Traditional calibration methods rely heavily on manual adjustments, which are time-consuming and prone to inaccuracies over time.*

WHAT DOES THIS STUDY ADD ON THIS TOPIC?

- *This study proposes an automated, machine learning-based calibration system for 16-bit resolvers, demonstrating a substantial reduction in angular error—from ±10% to ±2%—and enhanced tracking precision in servo-motor-controlled ground stations. The approach also reduces the goal angle error from 1° to as low as 0.2°, setting a new benchmark in resolver calibration performance.*

Corresponding author:
Ramiz Görkem Birdal

E-mail:
ramizgorkem.birdal@iuc.edu.tr

Received: December 30, 2024
Revision requested: February 18, 2025
Last revision received: March 4, 2025
Accepted: March 10, 2025
Publication Date: July 28, 2025

DOI: 10.5152/electrica.2025.24167

ABSTRACT

Resolvers are very accurate rotating position feedback mechanisms utilized by Low Earth Orbit (LEO) ground stations to track a satellite and communicate with it. Mechanical misalignments and temperature fluctuations are some of the environmental reasons that commonly cause resolvers to suffer from problems in calibration. The contribution of this work is to present a methodology for the calibration of 16-bit resolvers using 14 different Machine Learning (ML) techniques that improve the accuracy and reliability of LEO ground stations. Conventional calibration techniques include mechanical adjustment of the resolver for known inaccuracies. This often involves much manual refinement and recalibration to achieve any reasonable degree of accuracy. On the other hand, the proposed automatic calibration would reduce the need to routinely perform human calibration, thereby reducing wastage of time and other resources. Machine Learning statistical algorithms can learn from data and generalize to new data, including complex input-output mappings, and have made such error profiles and resolution features visible. This software-based error-compensation technique improved the target distortion ratio of a 16-bit resolver from approximately ±10% to approximately ±2%. In cases where ML is used for calibration, it is possible to reduce the goal angle error—which can reach up to 1°—to a level of 0.2°.

Index terms— Encoder, LEO ground stations, machine learning, resolver

I. INTRODUCTION

The main purpose of a Low Earth Orbit (LEO) ground station is to establish communication with satellites in the Earth's orbit. Since LEO spacecraft are traveling at rapid speed, the satellite ground stations need to target the satellite as precisely as possible in order to obtain the right telemetry information. This ensures that during orbit, feedback control mechanisms will keep the antenna in the correct orientation relative to the satellite. In relation to the satellites' ground stations, it is also a significant constituent, a feedback control system, which acts to accomplish the task of tracking and linking up with orbitally deployed satellites. These systems utilize the information supplied from sensors, such as resolvers, encoders, Global Positioning System (GPS), or Inertial Measurement Units, to make continuous adjustments in the position of the antenna based on deviations from the planned track. While they serve similar purposes, a number of factors might account for discrepancies in the degrees of rotation recorded by these devices. These are not limited to differences in accuracy and resolution, calibration and alignment issues, environmental effects, and mechanical wear. A resolver, on a satellite ground station's side, is not only one of the major parts of their feedback systems but it is also one of the main devices responsible for generating disagreement.

These electromechanical components, which give exact angular position feedback, become very important in the tracking systems of LEO ground stations. In most cases, a resolver is made up of a cylindrical rotor and stator for measuring the azimuth antenna (horizontal angle) and elevation (vertical angle). These are necessary measurements so that the antenna will be positioned precisely in order to monitor satellites crossing the cloud. Encoders, on the other hand, are technological devices used to convert mechanical motion into digital signals that can be read

by computer systems. The resolution of the encoders often creates digital outputs, while encoders also provide an analog signal, which represents the shaft angle. The passing of digital feedback on the position of the antenna is very much related to satellite ground stations, which are often provided by using encoders along with resolvers. The resolver and encoder work in such a manner that the ground station can monitor and interact with the satellites correctly. This ensures that the transmission and reception of data are dependable, ranging from various uses in telecommunications and Earth observation, to scientific research. While satellite tracking is initiated, the values for the azimuth and elevation of the antenna are provided by the resolvers. This is done when a ground station is set up for the very first time. The reference value that is obtained will serve as the starting point. Once this reference value has been obtained, there is a rotation mechanism involved according to where the satellite is located in the earth. Immediately after the tracking process is over, the resolver is once again used to get the reference location for the purpose of tracking a third satellite. However, since there is a variance in the resolver, the location information that is acquired may also be inaccurate. Again, even though an encoder can locate the degrees without any variation, after the motor has begun its rotation, it will not be able to find the final degree. Since the difference between the encoder and the resolver needed to be observed, both were set to the same value, and the operations were executed in parallel.

A. Literature Review

There have been a variety of missions that have led to the deployment of a large number of LEO satellites into near-earth space in recent years. These missions include space exploration [1, 2], Earth remote sensing [3, 4], monitoring of the weather [5], navigation augmentation [6, 7], worldwide telecommunications [8–10], and connectivity to the Internet of Things [11, 12]. As a result of their lower altitudes, LEO satellites provide a number of benefits that are not available with other methods of communication. These benefits include increased ground transmission power and less signal noise [13–14]. SpaceX and OneWeb are two examples of commercial companies that have suggested the construction of global LEO constellations [15]. These constellations would consist of hundreds of satellites and would enable access to the Internet on a worldwide scale. In tandem with the progression of this technology, the significance of satellite ground stations and sensors that are utilized in these systems will also increase. The shaft angle is translated into an analog signal using electromechanical means in one of these devices, which is referred to as a resolver [16–17]. In light of the substantial body of literature that provides evidence that resolver error patterns [18–21] are systematic, the implementation of a compensation technique to address this systematic mistake has the potential to significantly enhance the accuracy of the manufacturer's quotations. In order to lessen the amount of measurement error that occurred in these trials, a variety of modulation strategies and excitation signals were utilized. The numbers [22–23]. The calculation of the performance of the Linear Resolver is also discussed in certain articles [24–27]. By the way, recent advancements in the computing capacity of computers have resulted in a rapid rise in the theory and application of deep learning. Additionally, a great number of anomaly detection methods that make use of deep neural networks are beginning to appear [28–29]. It has been noted in recent years that machine learnings (MLs) have been used to solve a wide range of calibration problems related to low-cost particle sensors [30–31]. There has been a proposal to use One Dimensional Convolutional Neural Network calibration for low-cost carbon monoxide sensors, which is compared with several ML-based calibration techniques [32]. The goal of a different study is to develop a standardized calibration protocol that can be implemented at low cost and to evaluate different calibration algorithms [33]. A study carried out recently this year employed ML models for sensor calibration, including linear regression, gradient boosting regression, and random forest regression [34]. The results of another recent study demonstrate a variety of nonlinear models are derived from the sensor response to varying methane concentrations, temperatures, and humidity, as well as models with interaction terms [35].

Similar to the previous studies, this research aims to employ ML for developing an automated and adaptive calibration system for 16-bit resolvers. Besides enhancing tracking accuracy and reducing calibration errors, this new technology is bound to enhance the overall performance of LEO ground stations.

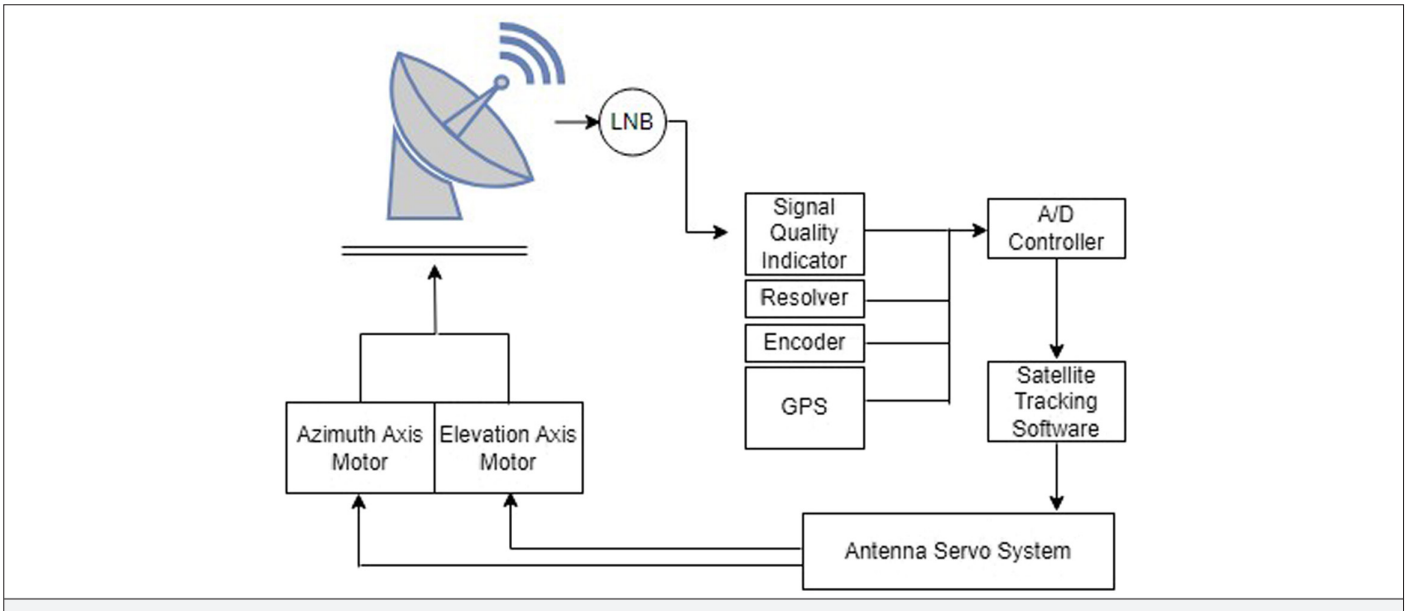

Fig. 1. The main control framework of satellite ground stations.

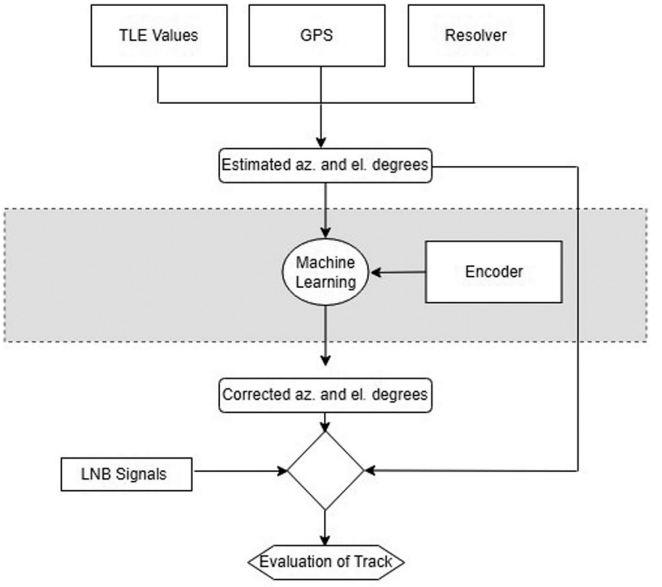

Fig. 2. ML-based approach to compensate for the faults made by the resolver.

The remainder of the article is structured in the following manner. The dataset, which serves as the model for measurements, is presented in the materials and methods section. In the third section, the implementation of the ML-based rectification procedure is presented. There is a discussion and evaluation of the results that were collected. A brief discussion of the potential future directions of this research is presented in the final section of this article.

II. MATERIALS AND METHODS

A. Dataset Collection

During the course of a track operation, resolver and encoder values were collected and assembled into the data set. In accordance with the results provided by the tracking algorithm of the satellite ground station, these are the two most important data points in which angular changes are monitored. In order for the tracking algorithm to correctly receive the signal from the next target angle, it is exceptionally vital that the values received from the resolver and encoder, which can be seen in Fig. 1, are taken into consideration. Due to the fact that the tracking process involves constant calculations, the objective is to conduct live calculations using the feedback from the sensors and the hardware, and then pay attention to any minor variations that may occur.

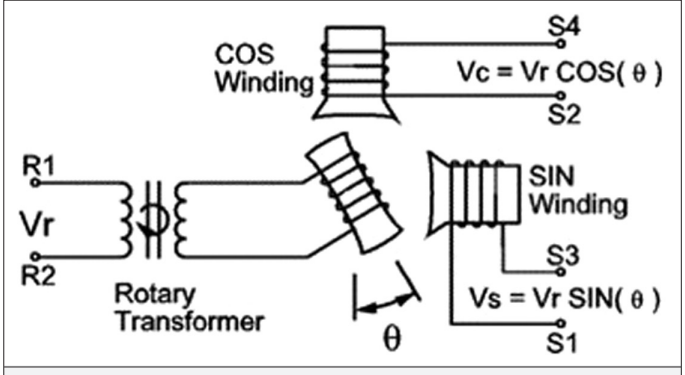

Fig. 3. Resolver schematic.

B. Machine Learning Models

In ML and statistical modeling, a variety of methods are employed to address both regression and classification tasks, each with distinct strengths. Decision trees offer interpretability through their hierarchical decision-making process, while k-nearest neighbors (kNN) relies on proximity-based classification, making it effective in low-dimensional spaces. Gaussian Processes (GPs) provide a probabilistic framework, capturing uncertainties in predictions, whereas robust methods like Theil-Sen and Huber Regressor mitigate the effects of outliers. Classical techniques like Linear Regression**,** Ridge Regression, and Lasso Regression address linear relationships, with Ridge focusing on multicollinearity and Lasso incorporating feature selection. Bayesian Ridge adds a probabilistic layer, while Elastic Net blends the penalties of Lasso and Ridge for enhanced flexibility. Linear Support Vector Regression (LSVR) and Random Forest handle complex, nonlinear patterns, with the former maximizing the margin of separation and the latter leveraging an ensemble of decision trees for greater accuracy. Passive Aggressive Regressors are efficient for online learning, adapting quickly to new data. Similarly, ensemble methods like the Bagging Regressor improve model stability by averaging predictions across multiple models. Following the application of these methods, calibration techniques ensure that model outputs are properly adjusted to align predicted values with actual outcomes, enhancing the reliability and interpretability of the results across diverse datasets.

In this paper, the top four methods that provided the best results based on the evaluation were selected. After applying a comprehensive set of ML algorithms, including regression and ensemble techniques, these four methods consistently outperformed the others in terms of accuracy, robustness, and predictive capability. The selection was made through a combination of model performance metrics and calibration, ensuring that the chosen models not only delivered high accuracy but also maintained reliability and stability across various test scenarios. A detailed description of these top-performing methods appears below, which forms the basis for further analysis and discussion.

1) Decision Tree:

A decision tree is a model that classifies data points based on their features using a tree structure consisting of nodes and branches. Each node represents a decision based on a specific feature, and the branches represent possible outcomes of the decision. The model works by traversing the tree to make predictions. The split at each node is based on criteria like Gini impurity (1) or entropy (2). The aim is to choose the feature that maximizes information gain.

$$G = 1 - \sum_{i=1}^{C} p_i^2 \tag{1}$$

$$H = -\sum_{i=1}^{C} p_i \log(p_i) \tag{2}$$

2) k-Nearest Neighbors:

The kNN is a simple algorithm that classifies a new data point based on the majority class of its kNN in the training data. The distance

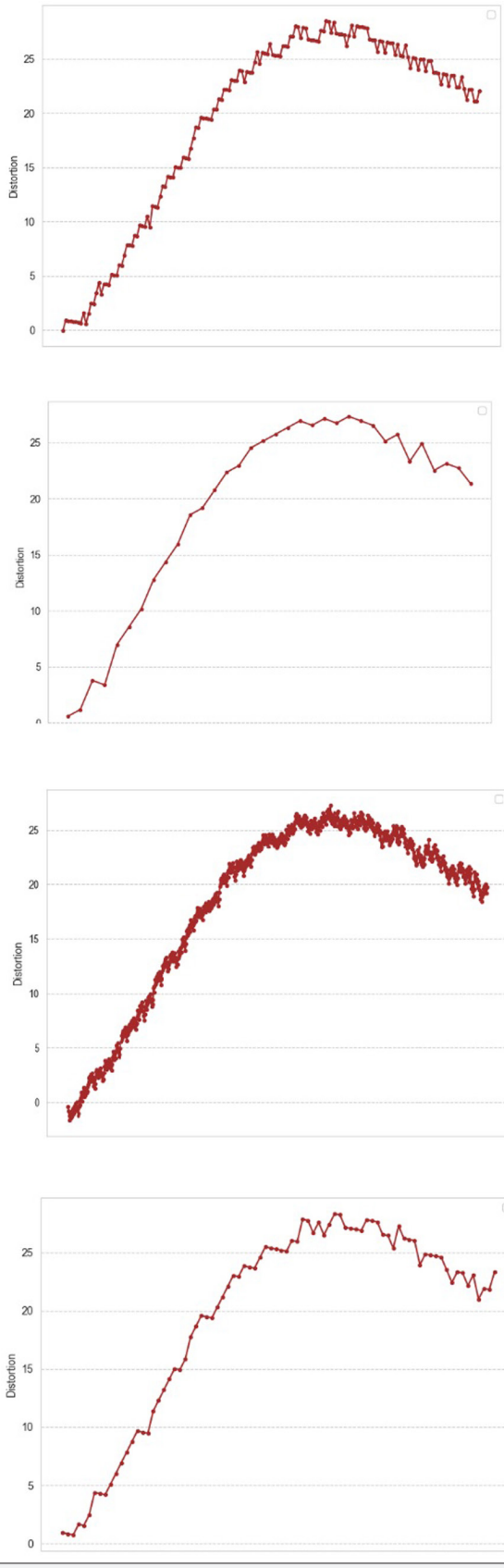

Fig. 4. Variations in the resolver value that occur during turning maneuvers of 0.2°, 1°, 2°, and 5° degrees.

between the new point and its neighbors is typically calculated using the Euclidean distance (3). The predicted class is determined by the majority vote of the neighbors.

$$d(x,y)=\sqrt{\sum_{i=1}^{n}(x_i-y_i)^2} \tag{3}$$

3) Gaussian Process:

A GP is a probabilistic model used for predicting continuous values. It assumes that the data follows a Gaussian distribution and models the relationships between data points using a covariance function, $k(x,x')$. Gaussian Process provides both the prediction and uncertainty for each prediction. A commonly used covariance function is the Radial Basis Function.

$$k(x,x')=\exp\left(-\frac{x-x'^2}{2l^2}\right) \tag{4}$$

4) Theil-Sen Estimator:

The Theil-Sen estimator is a robust regression method used to estimate the slope of a set of points. It computes the slope between all pairs of data points, then takes the median of these slopes as the final estimate. This method is resistant to the influence of outliers.

$$m_{ij}=\frac{y_j-y_i}{x_j-x_i} \tag{5}$$

C. Machine Learning-Based Compensation Algorithm

The presented compensation algorithm aims to reduce undesired disturbances and imperfections in systems in order to mitigate their effects. As a result of its enhanced ability to learn and correct imperfections, this ML-based compensation algorithm offers superior performance to traditional methods.

As it is seen in Fig. 2, Sensor data is fed into ML. The different models of ML have resolver, encoder, GPS, and TLE (Two-line element set) inputs and two corrected outputs. The compensation values between the estimated and corrected values are the outputs.

D. Resolver-To-Digital Converter

Electronic and mechanical devices known as resolvers as seen in Fig. 3 are utilized for the purpose of determining the angle at which a rotating shaft is pointed. As a result of their durability and dependability in hostile settings, they are frequently utilized in industrial applications, aircraft, and robotics. A Resolver-to-Digital Converter (RDC) is responsible for converting the analog sine and cosine signals into digital form, which allows for the digital computation of the rotor angle.

Stators have a resolver primary field winding (R1–R2) and a secondary magnetic field winding (S2–S4, S3–S1). Input into the primary winding is the excitation signal (R1–R2):

$$V_r=V_m\sin(wt) \tag{6}$$

V_m is the peak voltage of the excitation signal, ω is the angular frequency of the excitation signal, and t is time.

Stator winding voltages are calculated as follows:

$$V_s=kV_m\sin(\theta)\sin(\omega t) \tag{7}$$

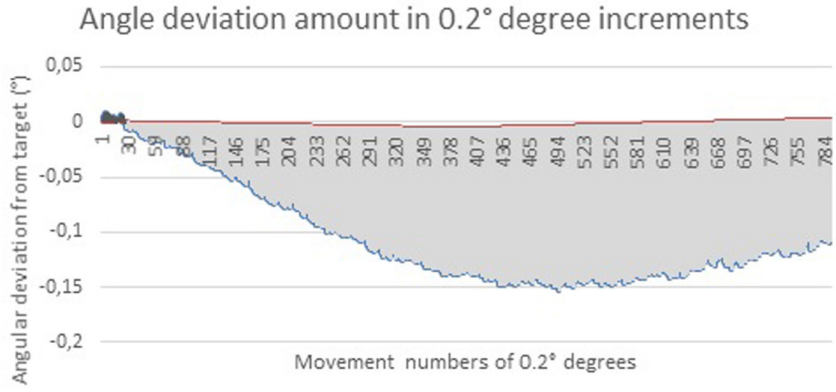

Fig. 5. The angle difference between the targeted and realized angle quantities for the resolver and encoder is quantified.

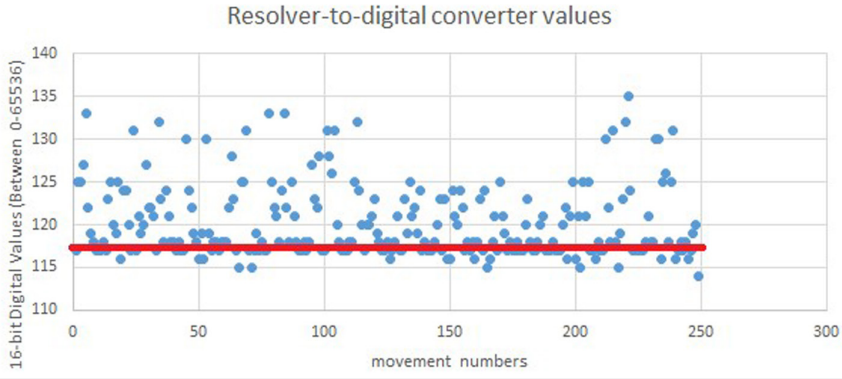

Fig. 6. The angle difference between the targeted and realized angle quantities for the resolver and encoder is quantified.

$$V_c = kV_m\cos(\theta)\sin(\omega t) \tag{8}$$

k is a constant relating to the resolver's design and θ is the rotor angle.

The following angle θ can be determined using sine and cosine outputs:

$$tan(\theta) = \frac{V_s}{V_c} = \frac{kV_m\sin(\theta)\sin(\omega t)}{kV_m\cos(\theta)\sin(\omega t)} = \frac{sin(\theta)}{cos(\theta)} \tag{9}$$

$$\theta = tan^{-1}\left(\frac{V_s}{V_c}\right) \tag{10}$$

E. Nanotec Servo Motor and Integrated Encoder

The Nanotec PD4 motor is a stepper motor that is known for its high level of precision and efficiency. It is frequently utilized in a variety of scientific and industrial applications. The motor is equipped with an encoder, which enables it to deliver precise feedback regarding position and speed. This is vital for achieving precise control and performance. The integrated encoder is a magnetic absolute encoder that functions with a single turn and has a revolution rate of 2000 encoder cycles. In addition, the gear ratio is equivalent to 10 000, which is the ratio of the revolutions of the encoder to the revolutions of the motor. By entering these numbers into the formula, the number of encoder increment values that increase by one degree for every degree of angle can be determined.

$$Encoder\ Increments = \frac{1}{360^\circ} \times 2000\,(encoder\ cycles\ per\ rev.) \times 10000\,(gear\ ratio) = 55555 \tag{11}$$

III. IMPLEMENTATION AND RESULTS

Throughout the process of data collection, satellite tracking was carried out by utilizing change commands of 0.2 degrees, 1 degree, 2 degrees, and 5 degrees. Throughout all of the studies, the motor movement was contrasted with commands that were either frequent, serial, or infrequent in order to determine how the movement changed. As can be seen in Fig. 4, these modifications led to the development of distinct methods for tracking satellites.

Fig. 5 demonstrates that a cumulative difference of up to 0.15 degrees has been recorded between the encoder, the resolver, and the target angle. This difference was observed at low angle ratios and during repeated rotation movements between the three locations. In the turning movement that is made with small angle values of 0.2 degrees and more frequent orders, it has been established that there is a deviation in the target tracking angles. This deviation is similar to the 2-degree angles that were shown in the previous graph.

TABLE I. PERFORMANCE COMPARISON OF MODELS: MEAN ERROR METRICS AND IMPROVEMENT RATES

Model	MSE	MAE	R^2	RMSE	MAPE
Linear Regression	25.25	4.50	0.9999995783	5.0249	0.0544
Ridge Regression	25.25	4.50	0.9999995783	5.0249	0.0544
Lasso Regression	25.25	4.50	0.9999995783	5.0249	0.0544
Elastic Net	30.25	4.75	0.9999994948	5.5	0.0671
Bayesian Ridge	25.25	4.50	0.9999995783	5.0249	0.0544
Huber Regressor	24.25	4.43	0.9999995950	4.9244	0.0535
Decision Tree	1.218	0.84	0.9999999796	1.1039	0.0091
Random Forest	72.78	7.96	0.9999987845	8.5311	0.0829
Linear Support Vector Regression	37.56	5.31	0.9999993727	6.1288	0.0556
K-Nearest Neighbors	1.781	1.09	0.9999999703	1.3346	0.0107
Gaussian Process	2.812	1.50	0.9999999530	1.677	0.0144
Theil-Sen	22.68	4.00	0.9999996211	4.7631	0.0485
Passive Aggressive	84.50	8.00	0.9999985888	9.1923	0.0716
Bagging Regressor	99.12	8.25	0.9999983446	9.9561	0.1047

These are the quantities of change that are a result of the rotational movement of the resolver with fixed angles, as can be seen in Fig. 6. In spite of the fact that the objective was to complete the rotation with 116 digital value movements displayed on the red line, it was not possible to achieve this objective in its entirety due to deviations. In order to provide an explanation for the equivalent of 116 digital values, the resolution of an RDC is determined by the number of bits that are present in its digital output. The resolution can be calculated using the following formula for a 16-bit RDC:

$Resolution = \frac{360^o}{2^{16}} \approx 0.0055^o$ To put it another way, a 16-bit RDC has the capability of distinguishing 65 536 discrete positions across an entire rotation of 360 degrees.

In order to maximize the performance of the system, it is essential to monitor the effectiveness of the compensation using a variety of different technologies. One way in which this was accomplished was by carrying out a comparative research, the results of which are presented in Table I. Upon examining the error metrics presented in Table I, it is evident that the R^2 values are consistently high across all models. However, there are significant variations in root mean square deviation, mean absolute percentage error , and mean absolute error metrics, which provide deeper insights into model performance. For instance, in the case of the kNN method, the MSE value is reported as 1.78, while the RMSE is calculated as 1.33. Since RMSE is the square root of MSE, this relationship is expected and confirms the consistency of the calculations. Similarly, for the LSVR method, the MSE is 37.56, with an RMSE of 6.13, maintaining the expected correlation. However, the differences in these error metrics across models highlight important performance insights. For example, models such as kNN and Decision Tree exhibit relatively low error values, suggesting strong predictive capabilities. On the other hand, ensemble methods like Random Forest and Bagging Regressor show significantly higher error values, indicating less accurate predictions in this specific scenario. Notably, the lowest MAE and MAPE values are observed in kNN and Decision Tree models, demonstrating their robustness and consistency in predictions. A more comprehensive comparison should consider MSE, RMSE, MAE, and MAPE collectively, ensuring that model selection aligns with the characteristics of the dataset and the specific requirements of the task.

TABLE II. RESIDUAL VALUES OF MODELS

Model	Mean Residual	Max Residual	Min Residual
Decision Tree	0.8438	2	0
K-Nearest Neighbors	1.0938	3	0
Gaussian Process	1.5000	3	0
Theil-Sen	4.0000	11	0

Table II shows the residuals for each of the top-performing models in the comparative study, showing the mean, maximum, and minimum residuals. Residuals are those values that indicate the difference between the predicted and actual values of a certain model. These give further detail on how error in any particular model will be distributed. The Decision Tree performed with the least mean residual at 0.8438, indicating that the actual values were slightly deviated from the expected values. K-nearest neighbors and GP, meanwhile, had relatively higher mean residuals; however, both were also a bit more consistent. Though the Theil-Sen had a mean residual of 4.0000, it nevertheless remained quite robust in dealing with non-linearities.

In addition to the residual data, a graph was constructed showing the distortion patterns of the predicted resolver values for the top-performing models. This graph provides a clear comparison between the predicted values for the Decision Tree, kNN, GP, and Theil-Sen models against the expected values Fig. 7. The following graph shows the compensating efficiency of the models against the distortions. The Decision Tree model kept minimal deviation from the expected values, while the kNN and the GP performed with much more sturdiness in the lines of minimal distortions. Another model that deformed due to the distortions slightly more was the Theil-Sen, but still, it managed to follow the general trend of the expected values. The above visual analysis reinforces the quantitative data and reiterates the desirability of ML-based methods in solving angular distortions. The closeness of their outputs to the expected values underlines their robustness and precision, especially in those environments where interference patterns are consistent.

IV. CONCLUSION

In conclusion, the utilization of a self-calibrating 16-bit resolver system for LEO satellite ground stations, which makes use of the ML technique, is a substantial advancement in terms of precision and dependability for satellite tracking and communication. When it comes to applications that require precise rotational position feedback in aircraft systems, encoders and resolvers are acknowledged to be essential components. Differences in their measurements might result in discrepancies in the functioning of the system, which necessitates an in-depth comprehension of the factors that are responsible

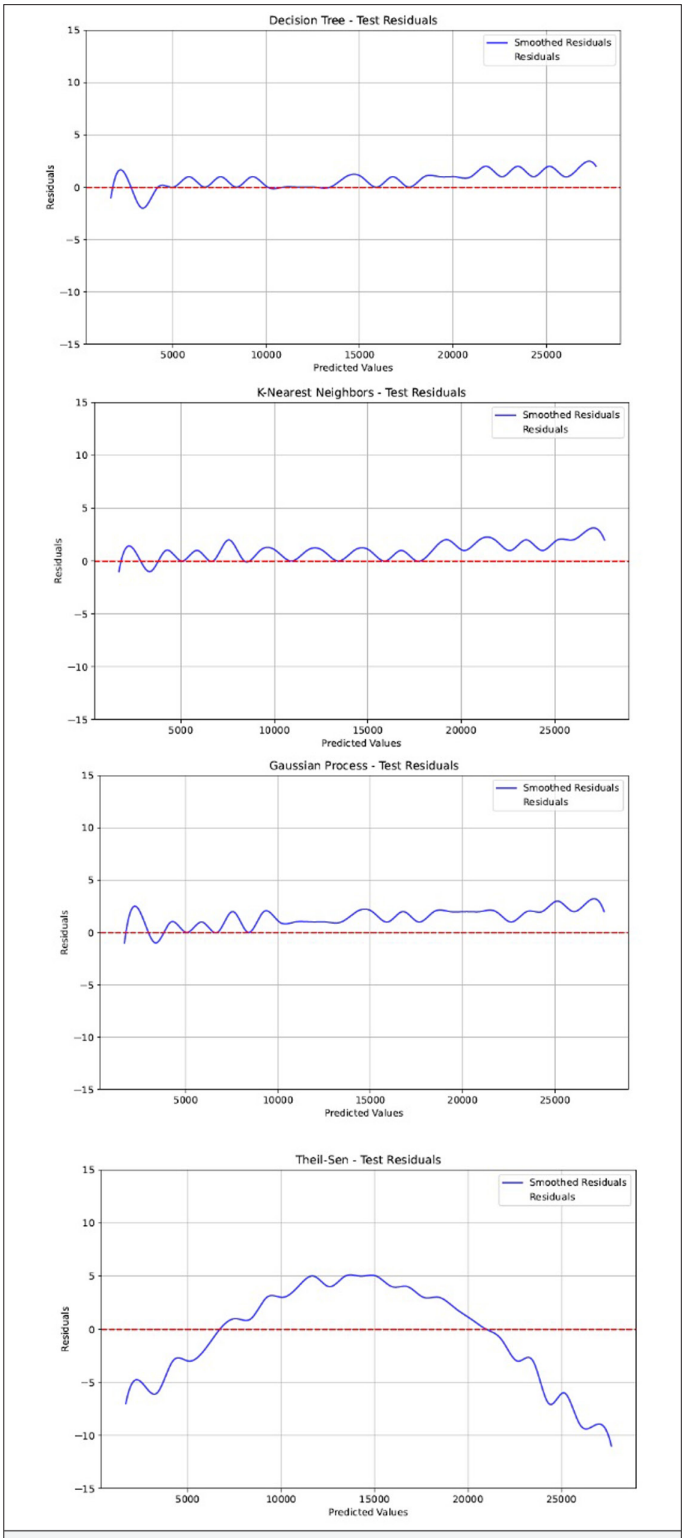

Fig. 7. Measurement of compensation using different techniques to compare performance.

for the inconsistencies. In this particular investigation, the ML correction resulted in a significant reduction in the disparities that existed between the degrees of rotation. By offering real-time, adaptive calibration, this new methodology tackles the inherent constraints of standard calibration methods, such as mechanical misalignment and environmental fluctuations. Specifically, this approach addresses these shortcomings. With its higher precision in angular position measurements, enhanced flexibility to dynamic situations, and decreased maintenance requirements, the ML-based system was able to display outstanding performance. Continuous learning and the ability to adapt to changing circumstances are two of the most important factors in ensuring sustained performance and precision, which are needed for the high demands of LEO satellite operations. In general, this self-calibrating technology not only enhances the efficiency and efficacy of ground station operations, but it also establishes a new benchmark for the advancement of satellite tracking technologies in the years to come. Future research should explore the integration of more advanced ML techniques, such as deep learning or reinforcement learning, to enhance adaptability in dynamic conditions. Additionally, expanding the system to multi-axis resolver applications could further broaden its usability in aerospace and robotics. Beyond satellite operations, this approach holds promise for real-world applications in autonomous navigation, industrial automation, and defense systems where precision and adaptability are crucial. These future advancements will contribute to the ongoing evolution of intelligent calibration technologies, ensuring sustained improvements in performance and reliability across various domains.

Data Availability Statement: The data that support the findings of this study are available on request from the corresponding author.

Peer-review: Externally peer-reviewed.

Author Contributions: Concept – X.X., X.X.; Design – X.X., X.X.; Supervision – X.X., X.X.; Resources – X.X., X.X.; Materials – X.X., X.X.; Data Collection and/or Processing – X.X., X.X.; Analysis and/or Interpretation – X.X., X.X.; Literature Search – X.X., X.X.; Writing – X.X., X.X.; Critical Review – X.X., X.X.

Declaration of Interests: Y.S. and R.G.B. have no conflict of interest to declare.

Funding: The authors declare that this study has received no financial support.

REFERENCES

1. S. Bandyopadhyay, R. Foust, G. P. Subramanian, S.-J. Chung, and F. Y. Hadaegh, "Review of formation flying and constellation missions using nanosatellites," *J. Spacecraft Rockets*, vol. 53, no. 3, pp. 567–578, 2016. [CrossRef]
2. S. Marcuccio, S. Ullo, M. Carminati, and O. Kanoun, "Smaller satellites, larger constellations: Trends and design issues for earth observation systems," *IEEE Aerosp. Electron. Syst. Mag.*, vol. 34, no. 10, pp. 50–59, Oct. 2019. [CrossRef]
3. G. Curzi, D. Modenini, and P. Tortora, "Large constellations of small satellites: A survey of near future challenges and missions," *Aerospace*, vol. 7, no. 9, p. 133, Sep. 2020. [CrossRef]
4. E. Peral et al., "Radar technologies for earth remote sensing from cubesat platforms," *Proc. IEEE*, vol. 106, no. 3, pp. 404–418, Mar. 2018. [CrossRef]
5. O. Kodheli et al., "Satellite communications in the new space era: A survey and future challenges," *IEEE Commun. Surv. Tuts.*, vol. 23, no. 1, pp. 70–109, 2021. [CrossRef]
6. X. Li, X. Guo, B. Zhu, and S. Geng, "Performance analysis of a navigation system combining BeiDou with LEO communication constellation," in China satellite navigation conference (CSNC) 2020 Proceedings: Volume II. Singapore: Springer, 2020, pp. 643–650. [CrossRef]
7. T. G. R. Reid, A. M. Neish, T. Walter, and P. K. Enge, "Broadband LEO constellations for navigation," *Navig. J. Inst. Navig.*, vol. 65, no. 2, pp. 205–220, 2018. [CrossRef]

8. B. Di, L. Song, Y. Li, and H. V. Poor, "Ultra-dense LEO: Integration of satellite access networks into 5G and beyond," *IEEE Wirel. Commun.*, vol. 26, no. 2, pp. 62–69, Apr. 2019. [CrossRef]
9. I. Leyva-Mayorga et al., "LEO small-satellite constellations for 5G and beyond-5G communications," *IEEE Access*, vol. 8, pp. 184955–184964, 2020. [CrossRef]
10. N. Saeed, A. Elzanaty, H. Almorad, H. Dahrouj, T. Y. Al-Naffouri, and M.-S. Alouini, "CubeSat communications: Recent advances and future challenges," *IEEE Commun. Surv. Tuts.*, vol. 22, no. 3, pp. 1839–1862, 2020. [CrossRef]
11. M. de Sanctis, E. Cianca, G. Araniti, I. Bisio, and R. Prasad, "Satellite communications supporting Internet of remote things," *IEEE Internet Things J.*, vol. 3, no. 1, pp. 113–123, Feb. 2016. [CrossRef]
12. Z. Qu, G. Zhang, H. Cao, and J. Xie, "Leo satellite constellation for Internet of Things," *IEEE Access*, vol. 5, pp. 18391–18401, 2017. [CrossRef]
13. B. Li, H. Ge, M. Ge, L. Nie, Y. Shen, and H. Schuh, "LEO enhanced global navigation satellite system (LeGNSS) for real-time precise positioning services," *Adv. Space Res.*, vol. 63, no. 1, pp. 73–93, 2019. [CrossRef]
14. R. S. Cassel, D. R. Scherer, D. R. Wilburne, J. E. Hirschauer, and J. H. Burke, "Impact of improved oscillator stability on LEO-based satellite navigation," In *Proceedings of the 2022 International Technical Meeting of the Institute of Navigation*, pp. 893–905. Available: https://doi, 2022. [CrossRef]
15. W. A. Hanson, "In Their Own Words: OneWeb's Internet constellation as described in their FCC form 312 application," *New Space*, vol. 4, no. 3, pp. 153–167, 2016. [CrossRef]
16. J. Gasking, Eds., *Synchro and Resolver Conversion*, 1980. Available: www.naii.comi.
17. Moog Components Group, *Synchro and Resolver Engineering Handbook*, 2004. Available: www.moog.comi.
18. D. C. Hanselman, "Resolver signal requirements for high accuracy resolver-to-digital conversion," *IEEE Trans. Ind. Electron.*, vol. 37, no. 6, p. 556–561, 1990. [CrossRef]
19. D. C. Hanselman, "Techniques for improving resolver-to-digital conversion accuracy," *IEEE Trans. Ind. Electron.*, vol. 38, no. 6, p. 501–504, 1991. [CrossRef]
20. L. Mingji, Y. Yu, Z. Jibin, L. Yongping, N. Livingstone, and G. Wenxue, "Error analysis and compensation of multipole resolvers," *Meas. Sci. Technol.*, vol. 10, no. 12, p. 1292–1295, 1999. [CrossRef]
21. N. Ukita et al., "A high-precision angle encoder for a 10-m submillimeter antenna," in *Publ. of the Natl Astron. Obs.* Japan, 2001.
22. Y. Hwang, and P. Jang, "New RDC method using trapezoidal excitation signal considering resolver nonlinearity," *IEEE Trans. Instrum. Meas.*, vol. 72, pp. 1–12, 2023.
23. P. Jang, T. Lee, Y. Hwang, and K. Nam, "Quadrature demodulation method for resolver signal processing under different sampling rate," *IEEE Access*, vol. 10, pp. 7016–7024, 2022. [CrossRef]
24. N. Nagasaka, Linear resolver'. US 4705971, 10 November 1987. Available: http://docs.google.com/viewer?url=patentimages.storage.googleapis.com/pdfs/US4705971.pdf. [accessed: December 2016].
25. Z. Nasiri-Gheidari, "Design, performance analysis, and prototyping of linear resolvers," *IEEE Trans. Energy Convers.*, vol. 32, no. 4, pp. 1376–1385, 2017. [CrossRef]
26. A. Daniar, and Z. Nasiri-Gheidari, "The influence of different configurations on position error of linear variable reluctance resolvers," 2017 25th Iranian Conf.Electrical Engineering (ICEE), Tehran, Iran, 2017, pp. 955–960. [CrossRef]
27. H. Tsujimoto, S. Tanaka, T. Shimono et al., "Design and analysis of are solver for 2DOF tubular motor," Industrial Electronics Society, IECON2016 – 42nd Annual Conf. IEEE, Florence, Italy, 23–26 October 2016.
28. K. Hundman, V. Constantinou, C. Laporte, I. Colwell, and T. Soderstrom, "Detecting spacecraft anomalies using lstms and nonparametric dynamic thresholding," in Proceedings of the 24th ACMSIGKDD International Conference on Knowledge Discovery & Data Mining, Ac. Med., New York, NY, pp.387–395, 2018.
29. H. Zhao, H. Liu, W. Hu, and X. Yan, "Anomaly detection and fault analysis of wind turbine components based on deep learning network," *Renew. Energy*, vol. 127, pp.825–834, 2018. [CrossRef].
30. M. Si, Y. Xiong, S. Du, and K. Du, "Evaluation and calibration of a low-cost particle sensor in ambient conditions using machine-learning methods," *Atmos. Meas. Tech.*, vol. 13, no. 4, pp. 1693–1707, 2020. [CrossRef]
31. S. Tondini, R. Scilla, and P. Casari, "Minimized training of machine learning-based calibration methods for low-cost O 3 sensors," *IEEE Sens. J.*, vol. 24, no. 3, pp. 3973–3987, 2024. [CrossRef]
32. S. Ali, F. Alam, K. M. Arif, and J. Potgieter, "Low-cost CO sensor calibration using one dimensional convolutional neural network," *Sensors (Basel)*, vol. 23, no. 2, p. 854, 2023. [CrossRef]
33. A. Wang et al., "Leveraging machine learning algorithms to advance low-cost air sensor calibration in stationary and mobile settings," *Atmos. Environ.*, vol. 301, 119692, 2023. [CrossRef]
34. R. Dubey et al., "Low-cost CO2 NDIR sensors: Performance evaluation and calibration using machine learning techniques," *Sensors (Basel)*, vol. 24, no. 17, p. 5675, 2024. [CrossRef]
35. H. L. Mitchell, S. J. Cox, and H. G. Lewis, "Calibration of a low-cost methane sensor using machine learning," *Sensors (Basel)*, vol. 24, no. 4, 1066, 2024. [CrossRef]

Yasin Sancar received the B.Sc. degree in Computer Engineering from Istanbul University in 2012 and PhD degree in Computer Engineering from Ataturk University in 2021. He is currently an academician at Erzurum Ataturk University. His research interests include embedded systems, optimization, image processing, and artifical intelligence.

Ramiz Görkem Birdal graduated with a B.Sc. degree in Computer Engineering from İstanbul University in 2012 and PhD degree in Computer Engineering from İstanbul University - Cerrahpaşa in 2023. He is currently an academician at İstanbul University - Cerrahpaşa. His research interests include biometrics, deep neural networks, satellite tracking systems, and electricity price forecasting.